Assessment of Electroosmotic Perfusion in Capillary Chromatographic Columns Using Electrical Conductivity

Patrick T. Vallano[†] and Vincent T. Remcho*

Department of Chemistry, Oregon State University, Corvallis, Oregon 97331-4003

Received: September 27, 2000; In Final Form: January 24, 2001

The electrical conductivity of capillary electrochromatography (CEC) columns packed with macroporous particles has been investigated. Columns were prepared with commercially available octadecylsilane-coated 7 μm diameter particles (Nucleosil) having nominal pore diameters of 100, 300, 500, 1000, and 4000 Å, and operated under typical CEC conditions. The conductivity of the 100 Å column was in agreement with that predicted from theory for nonporous spheres, indicating that intraparticle current was negligible. Columns packed with the wide-pore media (1000 Å and 4000 Å), in contrast, yielded conductivity values over 2-fold greater than the 100 Å. The electroosmotic contribution to current flow in these columns was deemed insignificant on the basis of theoretical modeling and the experimental data. It was therefore concluded that the increased column conductivity of the wide-pore packed columns was the result of intraparticle current transport. These results further suggest that wide-pore packings are more permeable to fluid flow and thus can provide maximum gains in efficiency due to electroosmotic perfusion when electrical double layer thickness is small relative to the median pore diameter of the packing.

Introduction

Capillary electrochromatography (CEC) is a chromatographic technique that employs electroosmosis, which is induced by an electric field applied along the column axis, as the driving force for bulk flow.[1−4] In their most common form, CEC columns consist of fused silica capillary tubes packed with conventional reversed phase HPLC particles (i.e., spherical silica particles 3−5 μm in diameter with < 100 Å pores). The technique is analogous to capillary HPLC with the exception that flow results not from a pressure gradient but from an electrical potential gradient. The principal advantage of CEC over capillary HPLC is the increased chromatographic efficiency, and accordingly, higher peak capacity, that arises from the intrinsic qualities of electroosmotic flow (EOF).

The desire to achieve even higher efficiencies and shorter analysis times has led to the use of macroporous HPLC particles in CEC under conditions such that flow through the pores of the particles occurs.[5,6] Intraparticle, or perfusive EOF can result in substantially increased efficiencies and shorter analysis times due to a decrease in the effective particle diameter and a smaller stagnant mobile phase contribution to plate height.[7]

The structure and uniformity of the packed bed are of critical importance to the performance of a chromatographic column, particularly with respect to band broadening. Variations in packing density between regions of the packed bed give rise to flow velocity induced broadening of peaks, one of the phenomena associated with eddy diffusion.[8] A highly variable packing structure amplifies this effect and can severely limit column performance. One of the advantages of packed column CEC over capillary HPLC is that the former is much less susceptible to this phenomenon. Under typical CEC operating conditions, EOF velocity is essentially independent of flow channel

diameter, and thus will vary only slightly between more or less densely packed regions of the column. Nevertheless, packing uniformity remains vitally important in CEC if efficiency and peak capacity are to be maximized.

The use of electrical conductivity measurements to characterize the packing structure of CEC columns has been reported recently by Wan,[9] who found that relative column conductivity, the ratio of packed bed to open tube conductivity, was a structural constant of the bed, dependent only upon the column porosity and tortuosity factor. The premise of the work was that because the particles are themselves nonconductive and, hence, current is due entirely to ion transport in solution, conductivity values can provide an indication of the "quality" of the packed bed. Unusually high conductivity suggests a loose packing structure and low values a collapsed bed or partial blockage. It was concluded that the conductive properties of the columns tested arose primarily from ion transport around the particles (i.e., in the interstitial region).

In an analogous manner, electrical conductivity may provide a useful tool with which to probe the flow permeability of the intraparticle region of a packed bed. Although the pore sizes of the particles used in the Wan paper were not specified, it would be expected that the extent of ion transport through the particles would increase with pore size. Furthermore, it is reasonable to expect that ion transport through macroporous particles that possess a large fraction of through-pores (i.e., pores providing a pathway through the particle) would contribute significantly to the conductivity of the packed bed. Relative to microporous columns of the same interstitial porosity for which current flow is primarily in the interstitial region, higher conductivities would be expected for the macroporous packed columns.

Typical macroporous packings are known to be heterogeneous with respect to pore size and structure. Electron microscopic analyses conducted by Tanaka et al.[10] and confirmed in our laboratory for macroporous Nucleosil particles produced by Macherey-Nagel (Duren, Germany) reveal that a single packing

* Corresponding author.
[†] Present address: Department of Drug Metabolism, Merck Research Laboratories, West Point, PA 19486.

consists of multiple subtypes of particles that vary in morphology. Information gleaned from the physical characterization of these packings as well as from packed column conductivity data could provide insight into the following: (1) the approximate pore diameter below which ion transport is minimal, and, potentially, above which pores act as "through-pores" and (2) differences in obstruction factors, perhaps arising from geometric effects such as tortuosity, that affect intraparticle current flow. The assumed operating principle is that the extent of intraparticle current transport in columns packed with macroporous particles could be useful in providing a measure of flow permeability *through* such particles under conditions where the double-layer thickness is small relative to the mean pore diameter.

Using the conductivity of a CEC column as a means to evaluate intraparticle permeability requires that the electroosmotic contribution to current flow, which results from ion transport within the electrical double layer, be small relative to the current flow in the bulk solution. To obtain a precise value of the electroosmotic current contribution in a packed column would be an exceedingly complex endeavor, thus in this work we make use of a simple model in which the column is treated as a bundle of parallel cylindrical capillary tubes of varying diameter, for which a series of equations describing current flow has been developed. As will be seen, the values predicted by the model in combination with the experimental data indicate that electroosmotic current can indeed be neglected in this study.

Theory

The magnitude of electrical current I_p transported through a tube packed with chromatographic particles is lower than that in an open tube I_o of the same diameter owing to two factors. First, a decrease in conductance results from a reduction in the free cross sectional area of the packed tube by a factor ϵ (the porosity) relative to an open tube. The conductance of the packed tube is further reduced by a decrease in effective ion mobility arising from geometrical constraints. As described by Boyack and Giddings,[11] this latter effect can be expressed in terms of a ratio of effective and free solution ion mobilities, termed the obstruction factor ξ, which includes a tortuosity term T and a constrictive factor C.

$$\xi = CT^{-2} \qquad (1)$$

The tortuosity term T^{-2} accounts for the reduction in effective migration rate due to nonalignment of flow channels with the field axis. This nonalignment acts to decrease the effective electric field strength and increase migration distance per unit displacement along the tube axis, hence the squared dependence on T. The constrictive factor C represents the reducing effect of channels of differing cross sectional area on electric field strength.

Accounting for these effects, the conductance of a packed tube G_p is decreased a factor $\epsilon\xi$ relative to an open tube of identical diameter G_o. In a chromatography column packed with nonporous particles, the total porosity ϵ_{tot} is equal to the interstitial porosity ϵ_i, thus

$$G_p = G_o\epsilon_i\xi \qquad (2)$$

Equation 2 can be written in terms of conductivity and rearranged as follows:

$$\frac{\kappa_p}{\kappa_o} = \epsilon_i\xi \qquad (3)$$

where κ_p and κ_o represent the conductivity of the packed and open tubes, respectively.

In practice, it is difficult to obtain precise values of C and T, thereby limiting the utility of eq 3. As a result, semiempirical relationships have often been used to describe the conductivity of porous media, in which the ratio κ_p/κ_o is usually expressed as a function of porosity.[12-15]

As in HPLC, most packing materials used in CEC are porous and as such transport of ions through as well as around the particles is possible. If macroporous packings are employed that possess a large fraction of through-pores compared to conventional porous particles, significant current flow through the particles might be expected. In such cases, where intraparticle as well as interparticle current transport is important, increased κ_p/κ_o values would result.

In the presence of electroosmotic flow (EOF), charge transport within the electrochemical double layer contributes to the total current in the CEC column. In their thorough treatment of electroosmosis in cylindrical capillary tubes, Rice and Whitehead derived the following expression for the magnitude of electroosmotic current.[16]

$$I_e = I_b \frac{(\epsilon_0\epsilon_r\zeta\kappa)^2}{\eta C\Lambda_b}\left[-1 + \frac{2I_1(\kappa a)}{\kappa a I_0(\kappa a)} + \frac{I_1^2(\kappa a)}{I_0^2(\kappa a)}\right] \qquad (4)$$

in which I_e is the electroosmotic current, I_b is the current in the bulk solution, ϵ_0 is the permittivity of vacuum, ϵ_r is the dielectric constant of the bulk solution, ζ is the zeta potential, κ is the reciprocal of the double layer thickness, ς is the solution viscosity, C is the molar concentration of electrolyte, Λ_b is the molar conductivity of the bulk solution, and a is the radius of the capillary tube. I_0 and I_1 are zero and first order, respectively, modified Bessel functions of the first kind. Equation 4 is limited by the use of the Debye–Hückel approximation for a (1:1) electrolyte and as such is valid only for low values (<100 mV) of ζ.

The ratio I_e/I_b, termed the relative conductivity λ, can be expressed in terms of the following equation, which was derived from the Rice and Whitehead equations by Wan.[17]

$$\lambda = \frac{2\epsilon_0\epsilon_r F^2}{\Lambda_b RT}\zeta^2\left[-1 + \frac{2I_1(\kappa a)}{\kappa a I_0(\kappa a)} + \frac{I_1^2(\kappa a)}{I_0^2(\kappa a)}\right] \qquad (5)$$

Estimations of λ for the different columns and eluent conditions employed in this study were obtained as follows. The general structure of a model previously published[7] was employed to calculate a volume averaged packed bed conductivity $\bar{\lambda}$. Briefly, pores with diameters ranging from 50 to 10000 Å were partitioned into 995 intervals of width 10 Å. From pore size distributions for the packings obtained by mercury intrusion porosimetry, the fraction of total column void volume contributed by each pore interval was determined. In these calculations, an interstitial porosity of 0.4 was assumed.[8] The volume fractions determined for the intervals and the interstitial region were subsequently used as weighting factors to obtain volume-averaged relative conductivity values for each column at each of the three buffer concentrations used. Treating each of the columns as comprising a bundle of capillary tubes of varying diameter, eq 4 was used to calculate the relative conductivity for each pore interval and for the interstitial space. The zeta potential was estimated for each column and buffer concentration from electroosmotic mobility measurements[18] and assumed to be equal on the outer particle surface and on surfaces within the pores. For the intraparticle pores, channel radius a was set

CEC Column Conductivity

J. Phys. Chem. B, Vol. 105, No. 16, 2001 **3225**

TABLE 1: Physical Dimensions of the Capillary Columns Used in This Study[a]

nominal pore diameter of packing (Å)	L_{bed} (cm)	L_{tot} (cm)
100	24.5	33.0
300	24.0	32.5
500	24.0	32.5
1000	24.0	32.6
4000	24.1	32.6

[a] All packings were Nucleosil ODS 7 μm particle diameter. For each column: i.d. = 75 μm, o.d. = 360 μm.

equal to the midpoint of the pore radius interval, e.g., pores in the diameter range 290−300 Å were assigned a = 295 Å. For the interstitial space, the relation d_{ch} = $0.28d_p$[16] was used to estimate channel diameter from particle diameter (d_p) assuming a uniform, well packed bed. Volume fraction weighting factors χ_v, calculated for each pore interval and the interstitial space were subsequently used in the determination of a volume averaged relative conductivity as indicated below.

$$\begin{array}{cc} \text{Intraparticle} & \text{Interstitial} \\ \text{Contribution} & \text{Contribution} \end{array}$$

$$\bar{\lambda} = \frac{\chi_{v1}\lambda_1 + ... + \chi_{v995}\lambda_{995} + \chi_{vint}\lambda_{int}}{\chi_{v1} + ... + \chi_{v995} + \chi_{vint}} \qquad (6)$$

Experimental Section

Concentrated hydrochloric acid (37%) was purchased from Mallinckrodt, St. Louis, MO. Ultrapure grade (99.9+%) tris-(hydroxymethyl) aminomethane (Tris) was obtained from Aldrich Chemical, Milwaukee, WI. HPLC grade acetonitrile was purchased from Fisher Scientific, Pittsburgh, PA. Water was thoroughly filtered and deionized using a Barnstead series 582 water purification system (Barnstead/Thermolyne Corporation, Dubuque, IA). Fused silica capillary tubing of 75 μm i.d., 360 μm o.d., was purchased from Polymicro Technologies, Inc., Phoenix, AZ. Nucleosil C18 silica particles (d_p = 7 μm) with nominal pore diameters of 100, 300, 500, 1000, and 4000 Å were obtained from Meta Chem Technologies, Torrance, CA.

The desired concentrations of Tris buffer were obtained by preparing a 100 mM solution of Tris (base form) adjusted to pH 8.0 by titration with concentrated HCl. This buffer solution was subsequently diluted in deionized H_2O to yield 50 and 25 mM solutions. The concentration of protonated TRIS (acid form), necessary for double layer thickness calculations, was estimated using the Henderson-Hasselbach equation (in this system, ionic strength I is essentially equal to the concentration of Tris in the acid form). Appropriate volumes of each buffer were mixed with acetonitrile to yield (20:80) (v/v) buffer/acetonitrile solutions, yielding final buffer concentrations of 20, 10, and 5 mM. These solutions were employed as eluents in the capillary electrochromatography experiments.

Packed capillary columns were prepared using a protocol reported previously.[7] The physical dimensions of the columns used in this study are provided in Table 1.

Current measurements were conducted using a Hewlett-Packard [3D]CE instrument (Hewlett-Packard Co., Waldbronn, Germany) equipped for external pressurization. During the runs, an external pressure of 5 bar was applied to the inlet and outlet mobile phase vials to minimize bubble formation within the capillary. A capillary temperature of 25 °C was maintained during the experiments. Current data was collected with the Hewlett-Packard Chemstation software package at a sampling

TABLE 2: Volume Averaged Relative Conductivity Values for the Packed Columns Calculated as Described in the Text

column	volume averaged relative conductivity		
	5 mM Tris	10 mM Tris	20 mM Tris
100 Å	0.018	0.013	7.2×10^{-5}
300 Å	0.029	0.020	0.0013
500 Å	0.038	0.012	7.2×10^{-5}
1000 Å	0.025	0.017	1.2×10^{-4}
4000 Å	0.024	0.015	9.2×10^{-5}

rate of 100 points min^{-1}. The data presented in the text represent the mean value of a minimum of 150 data points.

Pore size distributions of the Nucleosil packing materials were investigated by mercury intrusion porosimetry. These analyses were performed by Micromeritics Instrument Corporation (Norcross, GA) using a Micromeritics AutoPore mercury porosimeter. Analysis of the porosimetry data was performed using GraphPad Prism (GraphPad Software, Inc., San Diego, CA) and Microsoft Excel (Renton, WA) software. Scanning electron micrographs were obtained using an AmRay 3300 FE scanning electron microscope (AmRay, Bedford, MA).

Results and Discussion

As is the case with most CEC columns, the capillaries in this study consisted of a packed bed and an open section on which detection is performed. Because the total column conductivity κ_t is the directly measurable quantity in these experiments, it was necessary to determine κ_p, the conductivity of the packed bed, by indirect means. With the assumption that the current is uniform over the length of the capillary and that the system obeys Ohm's law, κ_p can be expressed in terms of measurable quantities as follows:

$$\kappa_p = \left[\frac{L_t}{L_p \kappa_t} - \frac{L_o}{L_p \kappa_o} \right]^{-1} \qquad (7)$$

in which L_t is the total column length, L_p is the packed bed length, L_o is the open section length, and κ_o is the conductivity of the open section. κ_o was determined through a separate set of experiments using an open fused silica capillary tube of the same internal diameter as the packed columns from the same lot of tubing.

At the outset, a review of the estimated contributions of electroosmotic conductivity is in order. In Table 2, volume-averaged relative conductivity values are presented. Most of the values are below 0.02 and in all cases are less than 0.04. At the highest Tris concentration of 20 mM, the relative conductivity values are 0.0013 or less for each of the columns. On this basis, it can be concluded that differences in κ_p/κ_o values are attributable primarily to ion transport in the bulk solution.

The κ_p/κ_o values obtained for the series of capillaries at Tris concentrations of 5, 10, and 20 mM are plotted in Figure 1. An important observation regarding the shape of the plots is that, within experimental error, the κ_p/κ_o ratio is essentially independent of Tris concentration, as evidenced by the shapes of the curves. This observation is critical in that it supports the assertion that electroosmotic conductivity is negligible under these conditions. Were it not, variation in the conductivity ratio with Tris concentration would be expected. Increasing the buffer concentration will compress the double layer, resulting in a decreased zeta potential (as well as an increased electrokinetic radius), which eqs 4 and 5 predict will affect the extent of electroosmotic current, specifically a decrease in λ with increasing Tris concentration due to the squared dependence
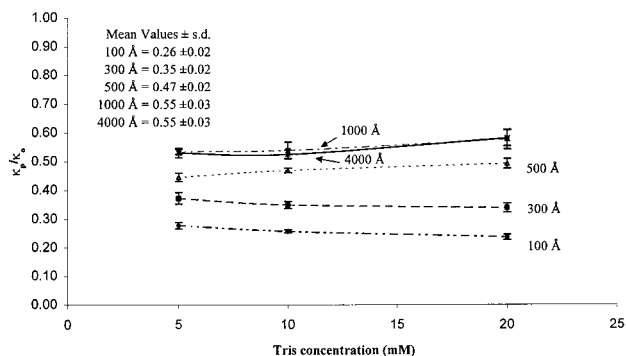
Figure 1. κ_p/κ_o values as a function of Tris concentration for the five packed capillary columns. Error bars indicate ± 1 standard deviation.

TABLE 3: Experimental and Theoretical κ_p/κ_o Values[a]

column	$(\kappa_p/\kappa_o)_{exp}$	$(\kappa_p/\kappa_o)_S$[b]	$(\kappa_p/\kappa_o)_{BG}$[c]	$(\kappa_p/\kappa_o)_{MT}$[d]
100 Å	0.26 ± 0.02			
300 Å	0.35 ± 0.02			
500 Å	0.47 ± 0.02	0.28[e]	0.26[e]	0.29[e]
1000 Å	0.55 ± 0.03			
4000 Å	0.55 ± 0.03			

[a] Theoretical Values Calculated Using the Equations below in Which $\epsilon_i = 0.4$ and $\theta = 1 - \epsilon_i$ [b] S = Slawinski equation:[12]

$$\frac{\kappa_p}{\kappa_o} = \frac{\epsilon_i}{(1.3219 + 0.3219\epsilon_i)^2}$$

[c] BG = Boyack-Giddings equation:[11,15]

$$\frac{\kappa_p}{\kappa_o} = \epsilon_i C T^{-2}$$

$$T = 1 + 0.173(1 - \epsilon_i)$$

$$C = (1 - \theta)^{-1}\left[\frac{1 + \theta}{(1 - \theta^{0.67})}\right]^{-1}$$

[d] MT = Meredith-Tobias equation:[14]

$$\frac{\kappa_p}{\kappa_o} = 8\frac{(2 - \theta)(1 - \theta)}{(4 + \theta)(4 - \theta)}$$

[e] Pore size independent values.

on ζ. The shapes of the curves permit the κ_p/κ_o values for each column to be averaged; these values are shown in the inset of Figure 1.

It can be seen that as the nominal pore size of the packing increases from 100 to 1000 Å, κ_p/κ_o values increase. Between the 1000 and 4000 Å packings, however, no noticeable difference exists. It is interesting to note that the κ_p/κ_o values for the widest pore media (1000 and 4000 Å) exceed those of the smallest (100 Å) by a factor of approximately 2. The fact that the nominal particle diameters of these packings are identical ($d_p = 7 \mu$m) and that the columns were packed using the same procedure allows the assumption to be made that the interstitial porosities of the five columns are essentially identical. On this basis, it can be concluded that the differences in the κ_p/κ_o values are due to the extent of intraparticle current flow. Comparison of these experimentally determined values with those predicted from various theoretical and semiempirical expressions derived for porous media consisting of hard spheres provides a method for testing this hypothesis.

Table 3 shows experimental κ_p/κ_o values in addition to those determined using three equations found in the literature. The calculated values were determined by neglecting particle porosity and assuming $\epsilon_i = 0.4$. Immediately apparent is that the 100 Å packing agrees quite well with each of the three calculated values. Additionally, the 100 Å data closely approach experi-
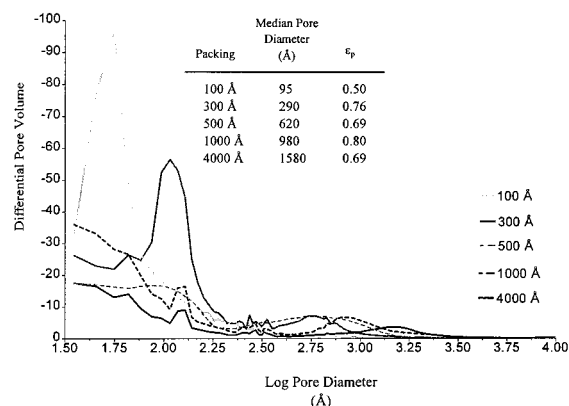

Figure 2. Pore size distributions for the packings determined by mercury intrusion porosimetry.

mental values obtained by Van Der Put and Bijsterbosch[19] for spherical polystyrene particles ($\kappa_p/\kappa_o = 0.28 \pm 0.02$). The agreement between these values implies that intraparticle ion transport is indeed negligible for the 100 Å packing. The larger pore sizes, however, differ significantly from the predicted conductivity values. It is evidently intraparticle current that results in the increased conductivities of the columns packed with larger pore particles.

In wide-pore media, the free cross-sectional area contributed by current-carrying pores will have the effect of increasing κ_p/κ_o. In this case, an effective total porosity ϵ_t' is needed to replace ϵ_i in eq 3. The effective porosity is greater than ϵ_i and simply represents the combined contributions of the interstices and the current carrying intraparticle through-pores to the overall free cross-sectional area. In principle, differences in intraparticle pore geometry and connectivity for the various packing materials could result in larger obstruction factors for some media, further increasing κ_p/κ_o.

It could be argued that the free cross sectional area available for current transport should be calculated based on the total column porosity ϵ_t. This, however, assumes that ion transport can occur in any pore, regardless of size or connectivity. Furthermore, the data obtained for the 100 Å column show that although the particles have a considerable porosity ($\epsilon_p = 0.5$ determined by mercury intrusion porosimetry), intraparticle current is negligible. Therefore, inclusion of pores in this size regime for this material would not yield an accurate method of normalization.

Although a precise assessment of pore connectivity in these packings would be at best a formidable task, pore size distribution data and κ_p/κ_o values can be used to estimate the diameter above which the intraparticle pores are likely to transport current. Intuitively, it would be expected that larger diameter pores have a greater probability of extending through the particles. Following this reasoning, packings with a greater fraction of large pores would be expected to yield higher values of κ_p/κ_o.

Pore size distributions for the packings determined by mercury intrusion porosimetry are shown in Figure 2. With the exception of the 100 Å media, the distributions are bimodal, having one maximum at approximately 120 Å and another at some larger diameter, the value of which varies with the material. The wide pore HPLC packings employed in this study have been shown to comprise a mixture of particle types;[10] the shapes of the distributions reflect the heterogeneity of the materials. From the pore size distribution data and Table 3, it is evident that κ_p/κ_o increases with the median pore size of the packings up to 1000 Å. No significant difference exists between the 1000 Å and 4000 Å columns. Interestingly, a median pore

CEC Column Conductivity

J. Phys. Chem. B, Vol. 105, No. 16, 2001 **3227**

TABLE 4: Intraparticle Pore Volume Fraction Contributed by Pores below Each Cutoff Diameter and Effective Total Porosity ϵ_t' Values for the Columns Employed in the Study

	intraparticle volume fraction below cutoff			ϵ_t'		
column	300 Å	500 Å	700 Å	300 Å	500 Å	700 Å
100 Å	0.78	0.84	0.88	0.47	0.45	0.44
300 Å	0.52	0.61	0.74	0.63	0.58	0.52
500 Å	0.28	0.40	0.56	0.70	0.65	0.58
1000 Å	0.26	0.30	0.35	0.77	0.75	0.72
4000 Å	0.18	0.22	0.24	0.75	0.74	0.72

diameter of approximately 1600 Å, significantly different from the nominal value, was determined for the 4000 Å packing. This likely accounts for the high degree of similarity in κ_p/κ_o values between the 1000 and 4000 Å columns.

These data allow the estimation of an "effective" total porosity, which, in addition to the interstitial volume, includes only the fraction of intraparticle void volume contributed by putative through-pores for each column. Values of effective total porosity ϵ_t' were determined by first selecting a cutoff pore diameter below which current transport was assumed to be negligible. It was shown previously that current flow in the 100 Å capillary occurs nearly exclusively in the interstitial region. Therefore, the pore size distribution of this packing was used as the basis from which to assign a cutoff point. Specifically, the range of pore sizes contributing most to the cumulative pore volume of the 100 Å pore size packing were assumed not to participate in current transport. To this end, and to evaluate results at different cutoff points, three cutoffs, at 300, 500, and 700 Å, were chosen. From the pore size distribution data, effective particle porosity ϵ_p' values were determined by neglecting the volume contribution of pores below the cutoff. Setting $\epsilon_i = 0.4$ and using the following relation, values of ϵ_t' were subsequently obtained.

$$\epsilon_t' = \epsilon_i + \epsilon_p' (1 - \epsilon_i) \tag{8}$$

In Table 4 the fraction of intraparticle pore volume contributed by pores below each cutoff diameter is shown for each packing material. Additionally, values of ϵ_t', calculated for each column by truncating at the appropriate pore diameter (300, 500, or 700 Å), are provided. Expectedly, the pore volume fraction below each cutoff is greatest for the 100 Å packing. For example, 84% of the cumulative pore volume falls below the cutoff diameter of 500 Å for the 100 Å packing, versus 22% for the 4000 Å material.

The effective total porosity values were next used to calculate obstruction factors for the columns. Rearranging eq 3 and substituting ϵ_t' for ϵ_i' yields the following expression for the obstruction factor.

$$\xi = \frac{\kappa_p}{\kappa_o \epsilon_t} \tag{9}$$

If the trends in experimental κ_p/κ_o values were due solely to differences in free cross-sectional area available for current flow, then any variation in obstruction factors for the five columns should be insignificant. Although the values presented in Table 5 do show a degree of convergence, they are seen to fall into two groups. At each cutoff, no difference exists, within experimental error, between obstruction factors for the 100 and 300 Å columns or the 500, 1000, and 4000 Å columns. Again invoking the assumption that intraparticle current in the 100 Å column is negligible, it is evident that the discrepancy in
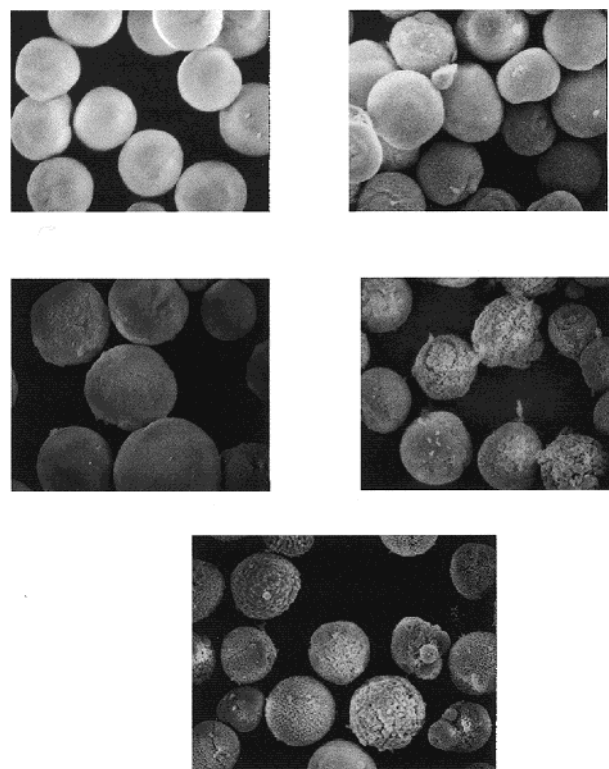
Figure 3. Scanning electron micrographs of the packing materials: (A) 100 Å, (B) 300 Å, (C) 500 Å, (D) 1000 Å, (E) 4000 Å.

TABLE 5: Obstruction Factors for the Capillary Columns

	$\xi \pm$ s.d		
column	300 Å cutoff	500 Å cutoff	700 Å cutoff
100 Å	0.55 ± 0.05	0.58 ± 0.05	0.59 ± 0.05
300 Å	0.56 ± 0.03	0.60 ± 0.04	0.67 ± 0.03
500 Å	0.67 ± 0.04	0.72 ± 0.04	0.81 ± 0.05
1000 Å	0.71 ± 0.04	0.73 ± 0.04	0.76 ± 0.04
4000 Å	0.73 ± 0.05	0.74 ± 0.05	0.76 ± 0.05

conductivity ratios cannot be accounted for by differences in free cross-sectional area alone.

Scanning electron micrographs of the packings are shown in Figure 3, in which the particle subtypes present in each material are visible. These images allow several important observations to be made. First, the particles comprising the packings can be divided into three general subtypes: narrow pore particles having a smooth appearance; intermediate pore size particles with a spongy appearance; and a wide pore subtype having a rough surface. Expectedly, the 1000 and 4000 Å media contain a significant fraction of the wide pore subtype. These particles appear to have a more open structure relative to the other subtypes and are absent in the other packings. The conductivity data, as well as the results of transmission electron microscopic analysis of these packings,[10] provide evidence that the wide pore subtype consists largely of through-pores. The 100 Å packing, in contrast, appears more homogeneous, consisting only of the smooth particles. These narrow pore smooth particles predominate in the 300 Å packing as well, although the intermediate subtype is also visible. Last, a mixture of smooth and intermediate pore size particles is found in the 500 Å packing. It is important to note that the fraction of smooth particles is less in the 500 Å packing than in the 300 Å. The conductivity data imply that current transport occurs through the intermediate particle subtype (i.e., to an appreciable extent, these pores behave as through-pores).

The differences in obstruction factors for the packings may be attributable to geometrical effects within the particle subtypes that comprise each packing material. The pores comprising the large-pore particle subtype found in the 1000 Å and 4000 Å packings may exhibit a decreased overall tortuosity and/or an increased constriction factor relative to the smaller pores in the intermediate subtype. This effect may be less pronounced for the intermediate pore size subtype of particle, resulting in the slightly smaller obstruction factor for the 500 Å column. The agreement in obstruction factors between the 100 and 300 Å columns is likely due to the fact that the extent of intraparticle current transport in the 300 Å column is relatively small. In this column, an insufficient fraction of particles having pores sufficient to allow current transport exists to have a discernible effect on the obstruction factor.

Conclusion

The results of this study indicate that macroporous packing materials support intraparticle current flow in chromatographic columns under typical CEC conditions. Columns packed with the widest nominal pore media, namely 1000 Å and 4000 Å, exhibited conductivities over 2-fold greater than that obtained for a column packed with conventional 100 Å pore diameter media, providing evidence of the existence of "through-pores" in these packings. The packed bed conductivity values and pore size distribution data obtained for the packing materials suggest that current transport is minimal through pores below approximately 300−700 Å in diameter. This value may represent the approximate diameter range above which pores have an increased likelihood of being through-pores. Obstruction factors determined separately by neglecting the volume contribution of pores below 300, 500, and 700 Å in diameter were highest for the columns packed with 1000 Å and 4000 Å media, possibly due to geometrical effects.

It can be concluded from these results that the 1000 Å and 4000 Å media yield packed beds with greater intraparticle flow permeability relative to the smaller pore media. These findings, in concert with results obtained from a thorough study of chromatographic efficiency of macroporous packed columns in the perfusive regime,[7] indicate that the use of these wide pore packings in CEC under conditions in which double layer thickness is small compared to the median pore diameter can serve to maximize gains in efficiency arising from electroosmotic perfusion.

References and Notes

(1) Knox, J. H.; Grant, I. H. *Chromatographia* **1987**, *24*, 135−143.
(2) Knox, J. H.; Grant, I. H. *Chromatographia* **1991**, *32*, 317−328.
(3) Dittmann, M. M.; Wienand, K.; Bek, F.; Rozing, G. P. *LC-GC* **1995**, *13*, 802−814.
(4) Vallano, P. T.; Remcho, V. T. *J. AOAC Int.* **1999**, *82*, 1604−1612.
(5) Li, D.; Remcho, V. T. *J. Microcolumn Sep.* **1997**, *9*, 389−397.
(6) Stol, R.; Kok, W. T.; Poppe, H. *J. Chromatogr. A* **1999**, *853*, 45−54.
(7) Vallano, P. T., Remcho, V. T. *Anal. Chem.* **2000**, *72*, 4255−4265.
(8) Giddings, J. C. *Dynamics of Chromatography* Marcel Dekker: New York, 1965.
(9) Wan, Q.-H. *J. Phys. Chem. B* **1997**, *101*, 8449−8453.
(10) Tanaka, N.; Hashidzume, K.; Araki, M.; Tsuchiya, H.; Okuno, A.; Iwaguchi, K.; Ohnishi, S.; Takai, N. *J. Chromatogr.* **1988**, *448*, 95−108.
(11) Boyak, J. R., Giddings, J. C. *Arch. Biochem. Biophys.* **1963**, *100*, 16−25.
(12) Slawinski, A. *J. Chim. Phys.* **1926**, *23*, 710−727.
(13) Bruggeman, D. A. G. *Ann. Phys.* **1935**, *24*, 636−664.
(14) Meredith, R. E., Tobias, C. W. *J. Electrochem. Soc.* **1961**, *108*, 286−290.
(15) Edward, J. T. *Adv. Chromatogr.* **1966**, *2*, 63−98.
(16) Rice, C. L.; Whitehead, R. *J. Phys. Chem.* **1965**, *69*, 4017−4024.
(17) Wan, Q.-H. *J. Phys. Chem. B* **1997**, *101*, 4860−4862.
(18) Schwer, C.; Kenndler, E. *Anal. Chem.* **1991**, *63*, 1801−1807.
(19) Van Der Put, A. G., Bijsterbosch, B. H. *J. Colloid Interface Sci.* **1980**, *75*, 512−524.